



Controlling the Twin Wire Arc Spray Process Using Artificial Neural Networks (ANN)

K. Hartz-Behrend, J. Schaup, J. Zierhut, and J. Schein

(Submitted May 21, 2015; in revised form September 18, 2015)

One approach for controlling the twin wire arc spray process is to use optical properties of the particle beam as input parameters for a process control. The idea is that changes in the process like eroded contact nozzles or variations of current, voltage, and/or atomizing gas pressure may be detected through observation of the particle beam. It can be assumed that if these properties deviate significantly from those obtained from a beam recorded for an optimal coating process, the spray particle and thus the coating properties change significantly. The goal is to detect these deviations and compensate the occurring errors by adjusting appropriate process parameters for the wire arc spray unit. One method for monitoring optical properties is to apply the diagnostic system particle flux imaging (PFI): PFI fits an ellipse to an image of a particle beam thereby defining easy to analyze characteristic parameters by relating optical beam properties to ellipse parameters. Using artificial neural networks (ANN), mathematical relations between ellipse and process parameters can be defined. It will be shown that in the case of a process disturbance through the use of an ANN-based control new process parameters can be computed to compensate particle beam deviations.

Keywords artificial neural network, coating quality, particle flux imaging, process control, twin wire arc spray

1. Introduction

Twin wire arc spray (TWAS) is a thermal spraying process with high cost efficiency and high deposition rates (Ref 1, 2). For providing a high quality coating it is necessary that a TWAS process is highly reproducible, but errors occurring during the coating process may influence the coating quality and thus the reproducibility of the coating results. The goal is to detect these errors and to compensate them by adjusting appropriate process parameters for the wire arc spray unit, i.e., the TWAS process needs to be monitored and controlled. One approach for doing this is to observe the spray particle beam and to detect deviations produced by process fluctuations during the spraying process.

In general, a significant change of the shape of the particle stream is a good indicator for a significant change of the coating properties. For monitoring the spray particle beam, the diagnostic system PFI can be applied which

will be described in the following section. Thus, the approach for a controlling of a TWAS process is based on controlling the shape of the particle beam. In case of a significant change of the particle stream it has to be “corrected.” This can be achieved by changing the process parameters of the wire arc spray unit. As a consequence of this, a link between numbers describing the particle beam (the monitored PFI data) and the process parameters is needed, i.e., a (mathematical) model is needed.

As will be seen in one of the next sections, non-linear dependencies can be identified between the monitored data and the process parameters. Therefore, a linear controller is usually not suitable for controlling the TWAS process. Additionally, since the properties of different TWAS units typically differ, mathematical models describing a link between the monitored PFI data and the process parameters typically differ, too. For these reasons, it would be nice if a model describing the link between the monitored data and the parameters could be found in an “easy” way. Hence, ANNs are used because ANNs can be trained by a number of experiments to find this link. In this way, it is not necessary to find an explicit model for describing the link.

In thermal spraying, ANNs are often used for modeling the behavior (Ref 3, 4) or for controlling atmospheric plasma spraying (APS) processes (Ref 5-7). Examples for a successful use of PFI in combination with ANN are given in (Ref 3, 4). A first application of ANNs in the area of wire arc spraying is given in Ref 8. The development of a neural network model in conjunction with arc spraying is also described in Ref 9 and 10.

The aim of this paper is to show that a TWAS process can be controlled using ANN. For this purpose, an ANN-based control is tested by artificially “disturbing” the process in different ways. As it will be seen, the ANN-

This article is an invited paper selected from presentations at the 2015 International Thermal Spray Conference, held May 11-14, 2015, in Long Beach, California, USA, and has been expanded from the original presentation.

K. Hartz-Behrend, J. Schaup, and J. Schein, LPT, Universitaet der Bundeswehr Muenchen, Werner-Heisenberg-Weg 39, 85577 Neubiberg, Germany; and J. Zierhut, Zierhut Messtechnik GmbH, Ruebezahlstrasse 19a, 81739 Munich, Germany. Contact e-mail: Joerg.Schaup@Unibw.De.

based control can compensate different kinds of process errors. Especially, it will be seen that process errors can be compensated the ANN was not trained for. Before the analysis of the ANN-based control is presented, the diagnostic tool PFI and analysis of the TWAS particle beam by means of this diagnostic tool will be introduced.

2. Particle Flux Imaging (PFI)

PFI is a diagnostic tool which is suitable for monitoring most thermal spraying processes, e.g., plasma spraying, arc spraying, or high velocity oxygen fuel spraying (HVOF) (Ref 11-13). PFI images show simultaneously the very bright carrier medium of the spray particles close to the gun and the less luminous particle flux in the downstream zone as provided by a CCD (charge-coupled device) camera. Carrier media may for example be the plasma jet and the HVOF jet. Due to the different luminosities of the carrier medium and the particle stream, two gray filters with different transmissions values are used for preventing overexposure of the CCD camera (Fig. 1).

A PFI image is generally divided into two parts, as shown in Fig. 2. Figure 2 (above) shows the carrier medium on the left-side and the particle flux on the right-side. The image is evaluated by finding intensity contours of constant gray scale values and fitting these lines to ellipses (Fig. 2, below).

Each ellipse in Fig. 2 is described by five key numbers (KN): the x - and y -position of the center point, the two semi-axes, and the angle between the x -axis and the major axis of the ellipse. It is also possible to use additional numbers for characterizing an ellipse, e.g., the average gray scale value of the pixels within an ellipse or the number of pixels within an ellipse in the PFI image (these values provide information about the luminosity of an approximated area in the image).

It is assumed that a change of the spraying conditions results in variations of the shape of the carrier medium and the particle jet. This in turn can be detected by the

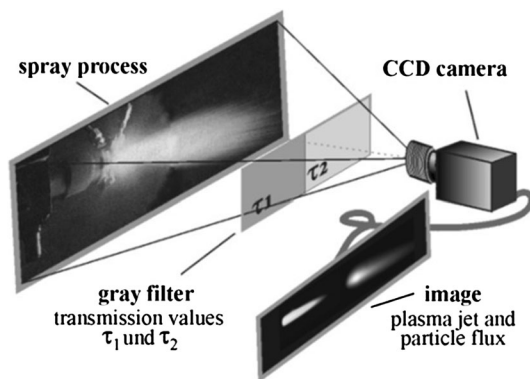


Fig. 1 Operating principle of the diagnostic system PFI. A CCD camera images simultaneously the carrier medium and the particle flux of a thermal spraying process. Due to the different luminosities, gray filters with different transmissions values τ_1 and τ_2 are used

PFI system providing characteristic KN values for each spray condition. By comparing the KN values of reference ellipses (defined for an optimized coating process) with ellipses for an ongoing coating process deviations from the optimum process can be detected.

3. Process Conditions

For the investigation, the spray gun “ArcSprayJetOne” from the company “T-Spray” (Lenningen, Germany) was used. As power source a gas metal arc welding (GMAW) power source from the company “EWM” (Oelsnitz, Germany), equipped with a second wire feeder, was applied in DC mode. For the DC process, the adjustable parameters of the power source are the voltage U and the wire feed rate v_w (proportional to the current). The advantage of the EWM power source is that its control acts very fast: it is able to adjust to new parameters during the spraying process very quickly (<1 s). The pressure P of the atomizing gas was set externally to 400 kPa. As atomizing gas, air was used and G3Si1 as spray wire (diameter 1.6 mm). In order to obtain appropriate images for the PFI image analysis, the exposure time was set to 5 s.

4. Statistical Investigation of a TWAS Particle Stream by Means of PFI

The investigation was performed by the method design of experiments (DOE). A full factorial 3^2 design including 2 repetitions for every parameter variation and additionally 3 repetitions at the central point was applied (so the full design consists of 21 parameter sets). The process parameter variations are shown in Table 1.

In the experiments, the focus was on the following KN values of the particle beam: the major axis a , the minor axis b , the average gray scale value of the pixels within an ellipse E_{avg} , and the number of pixels within an ellipse E_N as response variables.

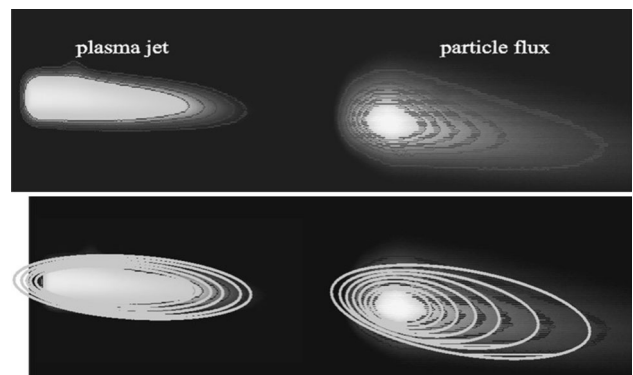
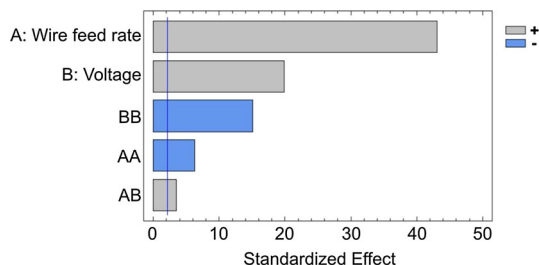


Fig. 2 Evaluation of a PFI image. Closed lines of constant gray scale values are fitted to ellipses (In this example, a PFI image of a plasma spraying process was taken for the evaluation)

Table 1 Parameter variations for the full factorial 3^2 design

Process parameters	Level 1	Level 2	Level 3
Voltage U , V	27	31	35
Wire feed rate v_w , m/min	3	5	7

**Fig. 3** Standardized Pareto chart of effects for the minor axis b (Color figure online)

As an example for the results of the PFI measurements in Fig. 3, a standardized Pareto chart of the influencing parameters for the minor axis b is given. It should be noted at this point that in a standardized Pareto chart a standardized effect is an effect (amount of change of a response variable caused by the variation of an input variable) divided by its standard deviation. From Fig. 3 it can be seen that, besides the factors U and v_w , also the factors U^2 , v_w^2 , and $U \cdot v_w$ have a statistically significant influence on the minor axis b of the particle flux ellipse. From the statistical analysis, the regression polynomial

$$b = -499.9 \text{ mm} + 9.249 \frac{\text{mm} \cdot \text{min}}{\text{m}} v_w + 30.43 \frac{\text{mm}}{\text{V}} U - 0.8 \frac{\text{mm} \cdot \text{min}^2}{\text{m}^2} v_w^2 + 0.2438 \frac{\text{mm} \cdot \text{min}}{\text{m} \cdot \text{V}} v_w U - 0.4778 \frac{\text{mm}}{\text{V}^2} U^2 \quad (\text{Eq 1})$$

with the coefficient of determination $R^2 = 0.9931$ was obtained.

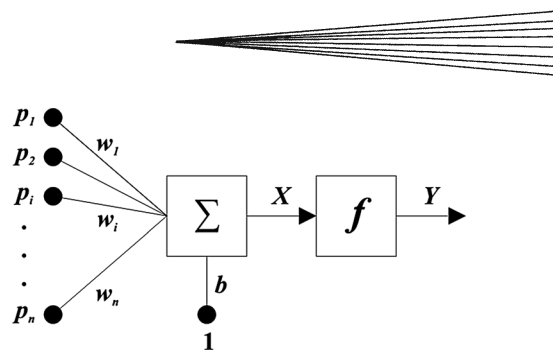
For the major axis a , the average gray scale value of the pixels within an ellipse E_{avg} and the number of the pixels within an ellipse E_N the regression polynomials are

$$a = -2501 \text{ mm} + 117.6 \frac{\text{mm} \cdot \text{min}}{\text{m}} v_w + 160.2 \frac{\text{mm}}{\text{V}} U - 14.2 \frac{\text{mm} \cdot \text{min}^2}{\text{m}^2} v_w^2 + 2.908 \frac{\text{mm} \cdot \text{min}}{\text{m} \cdot \text{V}} v_w U - 2.688 \frac{\text{mm}}{\text{V}^2} U^2 \quad (\text{Eq 2})$$

with $R^2 = 0.9985$,

$$E_{\text{avg}} = -200.6 - 1.700 \frac{\text{min}}{\text{m}} v_w + 19.45 \frac{1}{\text{V}} U + 0.1481 \frac{\text{min}}{\text{m} \cdot \text{V}} v_w U - 0.2856 \frac{1}{\text{V}^2} U^2 \quad (\text{Eq 3})$$

with $R^2 = 0.9981$ and

**Fig. 4** Graphical model of a perceptron

$$E_N = -290656 + 1224 \frac{\text{min}}{\text{m}} v_w + 17846 \frac{1}{\text{V}} U - 404.73 \frac{\text{min}^2}{\text{m}^2} v_w^2 + 272.49 \frac{\text{min}}{\text{m} \cdot \text{V}} v_w U - 290.65 \frac{1}{\text{V}^2} U^2 \quad (\text{Eq 4})$$

with $R^2 = 0.9916$.

Due to the high coefficient of determination, Eq 1-4 describe functional relations between the response variables a , b , E_{avg} , E_N , and the process parameter U , v_w very well. This leads to the conclusion that it should be possible to control the wire arc spraying process for the applied GMAW power source. It should be noted that all dependencies in Eq 1-4 are non-linear. Furthermore, in Eq 3, a v_w^2 -term is missing in comparison to the other Eq 1, 2, and 4.

5. An Artificial Neural Network for Controlling the TWAS Process

In the previous section it was seen that it should be possible to control the TWAS process based on the KN values obtained from particle flux. However, not all dependencies between the KN values and the process parameters are linear. This suggests that it might be advantageous to control the spraying process with an artificial neural network (Ref 14). For using an ANN, it is not necessary to know an explicit mathematical model for the relation between controlled variables and actuating variables: ANNs can be trained to find an adequate relation. For controlling, a function from the set of controlled variables to the set of actuating variables is needed (Eq 1-4 describe the converse relation).

An ANN is a model that is inspired by the functional principle of the human brain. It consists of nodes, so-called neurons, and a network that connects the neurons. For this research a multi-layer perceptron (MLP) was used as ANN. An MLP consists of perceptrons (Fig. 4).

The functionality of a perceptron is as follows: Each input (signal) p_i is multiplied by its weight w_i ; the weighted inputs are summed; and a bias b is added resulting in a sum X . X is put in a transfer function f and the result is the output Y . An MLP is feed-forward network organized in layers L_1, \dots, L_N . The layer L_1 is the input Layer; L_N is the

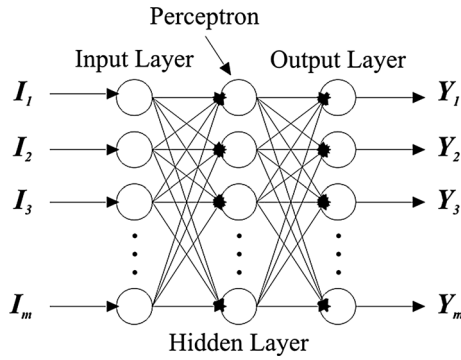


Fig. 5 Illustration of an MLP with one hidden layer

output layer; and the other layers are called hidden layers (Fig. 5). Only connections between L_i and L_{i+1} exist.

The calculation of the output of an MLP is simple: for each perceptron the output is calculated moving forward from layer to layer starting in the input layer. To train an MLP means to find weights and biases with a learning algorithm so that for a set of given inputs the sum of the squared differences between calculated and desired outputs is minimal. The performance of an MLP depends very much on the number of hidden layers and perceptrons.

For test purposes, the center point of the experimental design was defined as an optimal process parameter set ($U_{\text{opt}}=31$ V, $v_{w,\text{opt}}=5$ m/min). We used this set as an optimal parameter set because for these parameters, and in the area near to these parameters the wire arc spray process ran very stable. For this point, the average measured KN values are $a_{\text{opt}}=561.3$ mm, $b_{\text{opt}}=48.5$ mm, $E_{\text{avg,opt}}=142$, and $E_{N,\text{opt}}=21395$ which defined the reference. For each parameter, set i of the performed experimental design the relative deviations $\Delta a_{\text{rel},i}$, $\Delta b_{\text{rel},i}$, $\Delta E_{\text{avg,rel},i}$, $\Delta E_{N,\text{rel},i}$ (in percent) from the optimum parameters was obtained defined through

$$\Delta a_{\text{rel},i} = (a_i/a_{\text{opt}} - 1) \cdot 100 \quad (\text{Eq } 5)$$

$$\Delta b_{\text{rel},i} = (b_i/b_{\text{opt}} - 1) \cdot 100, \quad (\text{Eq } 6)$$

$$\Delta E_{\text{avg,rel},i} = (E_{\text{avg},i}/E_{\text{avg,opt}} - 1) \cdot 100 \quad (\text{Eq } 7)$$

$$\Delta E_{N,\text{rel},i} = (E_{N,i}/E_{N,\text{opt}} - 1) \cdot 100 \quad (\text{Eq } 8)$$

where a_i , b_i , $E_{\text{avg},i}$, $E_{N,i}$ are the original KN values (the standard PFI evaluation algorithm offers relative deviations as standard output when a reference ellipse is defined). The results of the 21 PFI measurements are shown in Fig. 6. For these measurements, each parameter set was measured individually. After initiation, the process was operated until a stable condition was reached and afterwards, one PFI measurement was done (acquisition time 5 s).

From Fig. 6, it can be seen that the charts of Δa , Δb , and ΔE_N have comparable shapes with different heights of the peaks. Therefore, the coefficients of correlation from the measurement data were calculated (Table 2).

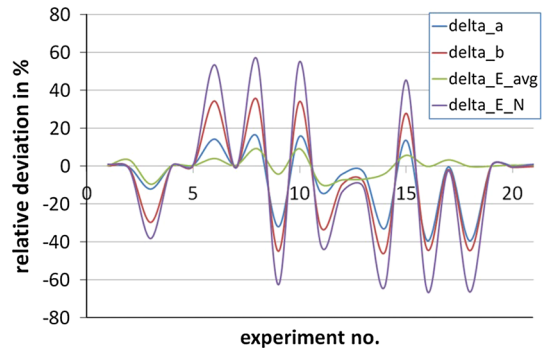


Fig. 6 Results of the 21 PFI measurements for Δa , Δb , ΔE_{avg} , ΔE_N (Color figure online)

Table 2 Coefficients of correlation for Δa , Δb , and ΔE_N

	Δa	Δb	ΔE_N
Δa	...	0.9577	0.9591
Δb	0.9577	...	0.9984
ΔE_N	0.9591	0.9984	...

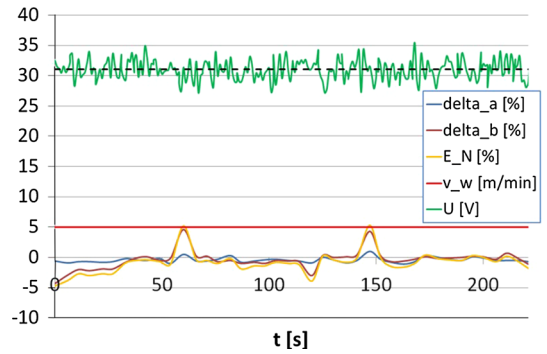


Fig. 7 Traces of Δa , Δb , and ΔE_N (also the traces of v_w and U are displayed). Process parameters were set to $U_{\text{opt}}=31$ V, $v_{w,\text{opt}}=5$ m/min (atomizing gas pressure $P=400$ kPa) (Color figure online)

As Table 2 indicates, the different coefficients of correlation are very high. This means (together with the charts in Fig. 6) that nearly linear dependencies exist between Δa , Δb , and ΔE_N . So it is sufficient to use only one of these three KN values for controlling the TWAS process. In order to decide which of these three values would be the best one for controlling, the different traces of Δa , Δb , and ΔE_N were compared when the process parameter set of the power source was set to the optimal set ($U_{\text{opt}}=31$ V, $v_{w,\text{opt}}=5$ m/min), Fig. 7.

Since TWAS is a thermal spraying process with a fluctuating particle beam, the PFI values fluctuate, too. From Fig. 7, it follows that the fluctuation for the KN value a is the lowest. As a consequence of this, a was used for controlling. In the case of using b or E_N a large peak like in Fig. 7 could imply a significant deviation from the reference ellipse and be interpreted as a process error by

the controlling algorithm even though the process is running smoothly. As second value, E_{avg} was utilized for the process control. For training the MLP, the relative deviations from the optimal parameters $\Delta a_{rel,i}$ and $\Delta E_{avg,rel,i}$ were used as input values for the MLP. Accordingly, the parameters $\Delta U_{diff,i}$ and $\Delta v_{w,diff,i}$ in Eq 9 and 10 were used as output values for the MLP.

This way, the MPL-based process control works as follows: When relative deviations Δa_{rel} and $\Delta E_{avg,rel}$ from the reference ellipse are measured, a deviation from the optimal coating process is detected. This deviation can be translated into changes ΔU_{diff} and $\Delta v_{w,diff}$ of the actual process parameters U_{act} and $v_{w,act}$ which can be calculated with the MLP. Therefore, the target process parameters are set to new process parameters ΔU_{new} and $\Delta v_{w,new}$ in Eq 11 and 12 in order to reach the optimal process parameters—as detected by the PFI—again.

$$\Delta U_{diff,i} = U_i - U_{opt} \quad (\text{Eq 9})$$

$$\Delta v_{w,diff,i} = v_{w,i} - v_{w,opt} \quad (\text{Eq 10})$$

$$\Delta U_{new} = U_{act} - \Delta U_{diff} \quad (\text{Eq 11})$$

$$\Delta v_{w,new} = \Delta v_{w,act} - \Delta v_{w,diff} \quad (\text{Eq 12})$$

For our investigations, we used a MLP with one hidden layer containing 5 neurons. In order to determine this, we investigated MLPs with maximal two hidden layers and maximal 7 neurons per layer. For each investigation, we used a different number of parameters sets for training the MLP. In order to avoid overfitting, the number of connections within the MLP. For example, a MLP with two hidden layers and 7 neurons per layer (2 inputs, 2 outputs) contains 77 connections. Therefore, we repeated our experimental design of 21 parameter sets four times to get enough data for training the MLP. For testing each MLP, we used always the same 10 parameter sets lying within a range where the wire arc spray process ran very stable. From all results, the MLP with one hidden layer containing 5 neurons delivered the best results concerning the mean squared error (MSE) and the testing data.

6. Different Tests of the ANN-Based Control

In order to test the ANN-based control, the process was artificially “disturbed” in different ways so that the particle flux ellipse differed from the reference ellipse. At first, the initial process parameters were set to parameters different from the optimal process parameters. Therefore, it could be verified if the ANN-based control adjusts the parameters back to the optimal parameters. For all performed tests, no substrate was coated and the wire spray gun was not moved.

In Fig. 8, an example of a disturbed process can be seen. The process was disturbed by setting the initial process parameters to $U = 36$ V and $v_w = 7$ m/min.

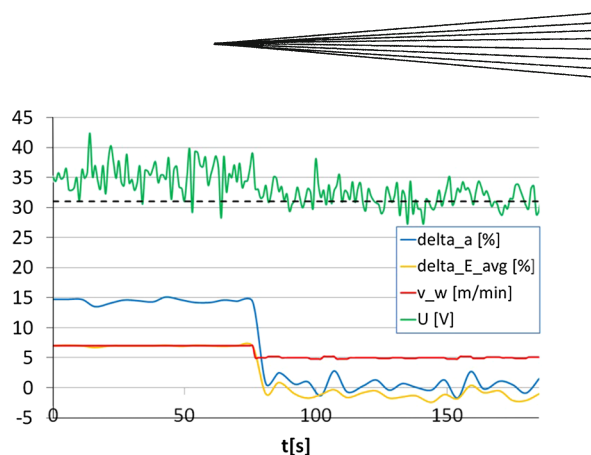


Fig. 8 Traces of Δa , ΔE_{avg} , v_w , and U for a disturbed process with activated ANN-based control. The control was activated after 76 s. The initial process parameters were set to $U = 36$ V, $v_w = 7$ m/min (atomizing gas pressure $P = 400$ kPa) (Color figure online)

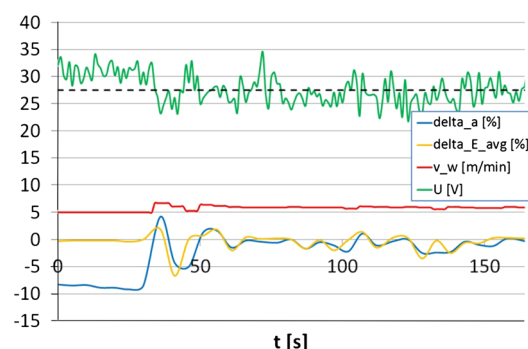


Fig. 9 Traces of Δa , ΔE_{avg} , v_w , and U for a disturbed process with activated ANN-based control. The control was activated after 30 s. The initial process parameters were set to the optimal process parameters $U_{opt} = 31$ V and $v_{w,opt} = 5$ m/min. The process was disturbed by setting the atomizing gas pressure to $P = 300$ kPa (Color figure online)

Figure 8 shows that the optimal process parameters $U_{opt} = 31$ V and $v_{w,opt} = 5$ m/min were reached again after the control was activated. Also, the KN values Δa and ΔE_{avg} are nearly fluctuating around 0 percent, which means that the ANN-based control for the GMAW power source works in principle.

For a second and a third test, the process was disturbed by setting the atomizing gas pressure P to 300 and 500 kPa, respectively (Fig. 9 and 10). The goal of this test was to find out how the ANN-based control can compensate errors it was not trained for.

Figure 9 shows that a lower pressure $P = 300$ kPa is compensated by setting the voltage to $U = 27$ V and the wire feed rate to $v_w = 6$ m/min. For Δa and ΔE_{avg} , the value 0 percent is not reached exactly: Δa is fluctuating around -0.8 and ΔE_{avg} around -0.5 percent. From Fig. 10 it can be seen that a higher pressure $P = 500$ kPa is compensated by adjusting the voltage to $U = 29.5$ V and the wire feed rate to $v_w = 4.5$ m/min. Furthermore, Δa is fluctuating around -1.2 and ΔE_{avg} around -0.3 percent. In both cases, the KN values $\Delta a = 0$ and $\Delta E_{avg} = 0$ of the reference ellipse were not reached exactly with activated ANN-based control but the new values were close to 0.

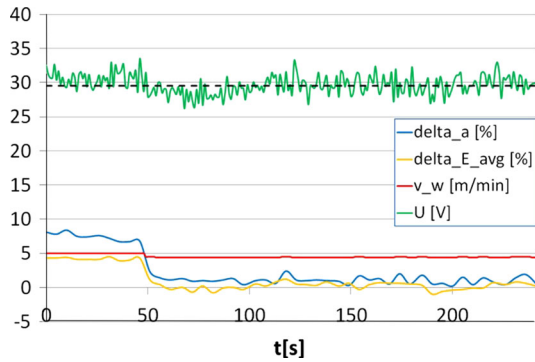


Fig. 10 Traces of Δa , ΔE_{avg} , v_w , and U for a disturbed process with activated ANN-based control. The control was activated after 46 s. The initial process parameters were set to the optimal process parameters $U_{\text{opt}} = 31$ V and $v_{w,\text{opt}} = 5$ m/min. The process was disturbed by setting the atomizing gas pressure to $P = 500$ kPa (Color figure online)

From the experiments it is known (compare with Fig. 7) that these deviations are in the order of “normal” fluctuations of a PFI ellipse for a TWAS process. Therefore, it can be stated that the reference ellipse was reached again with new process parameters. Now the question is, if different process parameters leading to particle beams with the same PFI parameters result in the same coating properties. The goal of future investigation is to find an answer to this.

7. Summary and Conclusion

In this paper, a method for controlling a TWAS process was presented. This method is based on the fact that a disturbance of the coating process results in a change of the properties of the spray particle stream. This change of properties can be recorded using the diagnostic system PFI which characterizes the particle stream on the basis of ellipses. Deviations from a reference ellipse defined for optimal coating parameters mean a deviation from the optimal process. Based on this, an ANN-based control was implemented using PFI ellipses numbers as input values.

In order to obtain images suitable for the PFI image analysis of a TWAS process, the exposure time has to be set to approximately 5 s. For the controlling of the process, a power source with a very quick controller is needed because the adjustment of the new parameters needs to be finalized before the next PFI image is acquired. If the controller of the power source were too slow, the process parameters would be changed too slowly and the new recorded shape of the particle beam would not correlate to the new parameters measured.

From different tests it can be seen that the ANN-based control can compensate different kinds of process errors, especially errors the ANN was not trained for: in the case of a lower or a higher atomizing gas pressure, the control found new values for the adjustable parameters voltage and wire feed rate of the power source so that the reference ellipse was reached again. But actually it is not

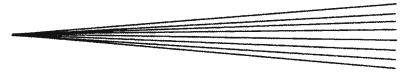
known if particle beams with the same PFI parameters result in the same coating properties. More investigations are needed.

Acknowledgments

Parts of this research and development project were funded by the German Federal Ministry of Education and Research (BMBF) within the Framework Concept “Research for Tomorrow’s Production” (funding Number 02PO2394) and managed by the Project Management Agency Karlsruhe (PTKA). The authors are responsible for the contents of this publication. For our investigations, we were also supported with a spray gun from the company T-Spray and with a power source from the company EWM. We thank the BMBF, the PTKA, T-Spray, and EWM.

References

1. L. Pawlowski, *The Science and Engineering of Thermal Spray Coatings*, Wiley, Chichester, UK, 1995
2. F.-W. Bach, A. Laarmann, and T. Wenz, Ed., *Modern Surface Technology*, Wiley, Weinheim, Germany, 2006
3. E. Lugscheider, F. Ernst, K. Seemann, T. Pfeifer, J. Dören, and J. Zierhut, Quality Control of Thermal Spray Processes Through Cost Effective Diagnostic Methods, *Thermal Spray 2005: Thermal Spray Connects: Explore its Surfacing Potential*, E. Lugscheider, Ed., Switzerland, DVS-ASM, 2005, p 1534-1539
4. A. Jakimov, M. Hertter, and H. Abdullahi, Plasma Spray Process Control with Neural Network, *Thermal Spray 2005: Thermal Spray Connects: Explore its Surfacing Potential*, E. Lugscheider, Ed., DVS-ASM, Basel, Switzerland, 2005, p 673-678
5. A.-F. Kanta, G. Montavon, M.-P. Planche, and C. Coddet, Artificial Intelligence Computation to Establish Relationships Between APS Process Parameters and Alumina-Titania Coating Properties, *Plasma Chem. Plasma Process.*, 2008, **28**(2), p 249-262
6. T.A. Choudhury, N. Hosseinzadeh, and C.C. Berndt, Artificial Neural Network Application for Predicting In-Flight Particle Characteristics of an Atmospheric Plasma Spray Process, *Surf. Coat. Technol.*, 2011, **205**(21-22), p 4886-4895
7. R.B. Heimann, Better Quality Control: Stochastic Approaches to Optimize Properties and Performance of Plasma-Sprayed Coatings, *J. Therm. Spray Technol.*, 2010, **19**(4), p 765-778
8. K. Hartz-Behrend, J. Schein, D.P. Jonke, M. Enghart, and J. Zierhut, Control of Wire Arc Spraying Using Artificial Neural Networks for the Production of Thin-Walled Moulds for Carbon Fiber Reinforced Plastics, *Thermal Spray 2012: Air, Land, Water and the Human Body: Thermal Spray Science and Applications*, R.S. Lima, A. Agarwal, M.M. Hyland, Y.-C. Lau, C.-J. Li, A. McDonald, and F.-L. Toma, Ed., ASM International, Houston, Texas, 2012, p 436-441
9. A. Khudhair, N.A. Talib, Neural Network Analysis for Sliding Wear of 13% Cr Steel Coatings by Electric Arc Spraying, *First Engineering Scientific Conference, College of Engineering—University of Diyala, Diyala Journal of Engineering Sciences*, 22-23 December, 2010, p 157-169
10. Y. Korobov, S. Nevezhin, V. Verkhorubov, G. Rimer, A. Zhilin, Optimization of Alloying of Heat Resistant Core Wires for Arc Spraying by Neural Network Modeling, *Thermal Process Modeling: Proceedings from the 5th International Conference on Thermal Process Modeling and Computer Simulation*, B.L. Ferguson, R. Goldstein, R. Papp, Ed., June 16-18, (Orlando, Florida), ASM International, 2014, p 323-328
11. K.D. Landes, T.V. Streibl, J. Zierhut, Particle Flux Imaging (PFI) and Particle Shape Imaging (PSI)—Two Innovative Diagnostics



- for Thermal Coating. *International Thermal Spray Conference*, E. Lugscheider and C.C. Berndt, Ed., March 4-6, (Essen, Germany), DVS Deutscher Verband für Schweißen, 2002, p 47-51
12. J. Zierhut, W. Pellkofer, A. Sagel, T. Haug, and K.D. Landes, Verification of Particle Flux Imaging (PFI) an In-Situ Diagnostic Method, *Thermal Spray 2001 New Surfaces for a New Millennium*, 28-30, C.C. Berndt, Ed., ASM International, Singapore, 2001, p 787-790
 13. J. Zierhut, K.D. Landes, W. Krömmer, and P. Heinrich, Particle Flux Imaging (PFI) In-Situ Diagnostics for Thermal Coating Process, *Thermal Spray: Surface Engineering via Applied Research*, May 8-11, 2000, C.C. Berndt, Ed., ASM International, Montréal, Québec, 2000, p 63-66
 14. M. McCord Nelson and W.T. Illingworth, *A Practical Guide to Neural Nets*, Addison Wesley, New York, 1991